Title
Thermal Conductivity of Municipal Solid Waste from In Situ Heat Extraction Tests

Journal
Journal of Geotechnical and Geoenvironmental Engineering, 146(9)

ISSN
1090-0241

Authors
Nocko, Leticia M
Botelho, Keaton
Morris, Jeremy WF
et al.

Publication Date
2020-09-01

DOI
10.1061/(asce)gt.1943-5606.0002325

Peer reviewed

Thermal conductivity of municipal solid waste from in-situ heat extraction tests

Leticia M. Nocko, M.S.[1], Keaton Botelho, M.S.[2], Jeremy W.F. Morris, Ph.D., P.E.[3],

Ranjiv Gupta, Ph.D., P.E.[4] and John S. McCartney, Ph.D., P.E., F.ASCE[5]

Abstract: As municipal solid waste (MSW) in landfills can reach temperatures greater than 50°C that may be sustained for several decades due to methanogenic bacteria activity, the generated heat is an alternative energy source that can be exploited for direct heating of nearby infrastructure or for augmenting industrial processes. However, in-situ measurements of MSW thermal properties are needed to properly design heat extraction systems for landfills. In this study, the spatial and temporal evolution of the waste temperatures in a new MSW landfill cell in Santee, California were monitored over 13 months. After the temperatures reached stable values, a 17-day heat extraction thermal response test was performed on serpentine geothermal heat exchangers that were installed at three elevations in the cell during waste placement. As the serpentine segments were separated from each other to minimize thermal interference during the heat extraction test, the pipes were assumed to represent line heat sinks. The values of effective thermal conductivity estimated from infinite line source analyses ranged from 0.86 to 1.32 W/m°C , which are consistent with values on the higher range of those from laboratory tests on MSW.

Keywords: Municipal solid waste, landfill, thermal response test, heat extraction, thermal conductivity.

[1] Graduate Research Assistant, Dept. of Structural Engineering, University of California San Diego, 9500 Gilman Dr. La Jolla, CA 92093-0085. lnocko@eng.ucsd.edu.
[2] Senior Engineer, Geosyntec Consultants, 16644 West Bernardo Drive, Suite 301, San Diego, CA 92127. KBotelho@geosyntec.com.
[3] Principal, Geosyntec Consultants, 1220 19th St. NW, Suite 210, Washington, DC 20036. JMorris@geosyntec.com.
[4] Senior Engineer, Freeport McMoRan, 333 N. Central Avenue, Phoenix, AZ 85004. rgupta2@fmi.com.
[5] Professor and Department Chair, Dept. of Structural Engineering, University of California San Diego, 9500 Gilman Dr. La Jolla, CA 92093-0085. mccartney@ucsd.edu.

INTRODUCTION

The decomposition of organic matter present in municipal solid waste (MSW) landfills generates heat leading to increase in temperature (Rees 1980a and 1980b; Young 1992; Yeşiller et al. 2005). Biodegradation of MSW under the moist, mesophilic and anaerobic conditions that generally exist within landfills can sustain temperatures significantly above ambient conditions for several decades. Biodegradation of MSW also contributes to the generation of leachate and landfill gas (LFG), predominantly methane and carbon dioxide (Poland and Harper 1986). The heat generated from biodegradation processes is an alternative energy resource that can potentially be extracted from the waste mass and used for direct heating of nearby facilities (Emmi et al. 2016). Further, heat extraction from the waste mass may permit engineered modification of processes in landfills. For example, Coccia et al. (2013) summarized several potential effects of heat extraction from landfills, including: (i) maximizing LFG capture for electricity generation by maintaining stable mesophilic temperatures to optimize microbial methane generation (Farquar and Rovers 1973; Rees 1980a); (ii) reducing the temperature gradient across the landfill base liner to minimize the potential for clay liner desiccation (Southen and Rowe 2005) or geomembrane damage (Jafari et al. 2014b); and (iii) exploiting the increased waste settlement rate observed at higher temperatures due to higher decomposition rates (e.g., Lamothe and Edgers 1994; Bareither et al. 2012) to maximize the landfill disposal capacity. To achieve any of these objectives in a controlled manner, in-situ characterization of the thermal properties of the waste mass is a key requirement.

This paper presents results from a heat extraction thermal response test on horizontal geothermal heat exchangers installed at different elevations in a new MSW landfill cell in Santee, California. Different from previous studies that explored the use of geothermal heat exchangers in MSW (e.g., Faitli et al. 2015a; Yeşiller et al. 2016; Shi et al. 2018), this study employs a chiller to provide a controlled heat extraction rate needed for in-situ thermal property estimation. The results from the heat extraction tests are used to estimate the in-situ effective thermal conductivity of the waste and heat exchange system using the line source analysis (Mogensen 1983; Gehlin and Hellstrom 2003; Sanner et al. 2005, 2008; Raymond et al. 2011; Stauffer et al. 2013; Murphy et al. 2014). Embedded instrumentation in the MSW landfill cell was used to evaluate the spatial and temporal evolution of temperature inside the cell during a 13-month period of self-heating of the MSW due to biodegradation, as well as during the 17-day heat extraction thermal response test.

BACKGROUND

The main byproducts of MSW biodegradation in landfills are leachate, biogas, and heat. The relative quantity of each byproduct generated is dependent on the specific waste composition and the stage of biodegradation observed within the MSW (Barlaz et al., 1990; Christensen et al. 1992; Baldwin et al. 1998; Staley and Barlaz 2009). Landfill biodegradation of organic matter is initially dominated by an aerobic stage, lasting from a few weeks to two years, followed by an anaerobic stage, which can last several decades (Bookter and Ham 1982; Kjeldsen et al. 2003). Yeşiller et al. (2005, 2015) observed that the rapid increase in temperature during the aerobic phase corresponds to approximately 20 to 30% of the total increase in temperature in the landfill, while the remaining 70 to 80% of the increase in temperature occurs during the anaerobic phase. In the anaerobic phase, the slow increase in temperature can be sustained for several decades as long as organic material is available for consumption.

Due to the growing interest in heat extraction from landfills in the past several years, either for direct use of the heat or for temperature control to optimize processes within the waste cell, several studies have been conducted to describe the temperature evolution and profile in MSW landfills. With respect to maximum temperatures, Yeşiller et al. (2005) observed values of 57, 35, 23 and 42 °C at MSW landfills in Michigan, New Mexico, Alaska, and British Columbia, respectively, while Rees (1980a) observed a maximum of 43 °C for a MSW landfill in the United Kingdom. Bouazza et al. (2011) reported average peak temperatures as high as 60 °C for a cell filled with organic waste in a landfill near Melbourne, Australia, and Lefebvre et al. (2000) measured a maximum temperature of about 55 °C in a landfill cell with industrial waste and MSW in France. Faitly et al. (2015a) measured temperatures as high as 55 °C in monitored MSW landfill in Hungary. Shariatmadari et al. (2011) compared the temperature evolution of two MSW cells in a landfill in Tehran, Iran (one with leachate recirculation and one without) and observed maximum monthly average temperatures of 60 °C and 54 °C, respectively. Processes such as air intrusion or exothermic chemical reactions in reactive waste (e.g., aluminum production waste) have been reported to lead to waste temperatures of 100 °C or more, sometimes corresponding to smoldering combustion (Stark et al. 2012; Jafari et al. 2014a and 2017). Although elevated heat generation and accumulation is currently of considerable research interest (e.g., Hao et al. 2017), this paper is focused on landfills within the typical mesophilic range for anaerobic biodegradation noted above.

In addition to reporting maximum waste temperatures, several studies have been conducted to identify the temperatures distribution within MSW cells during the biodegradation process. The temperature profile most frequently observed in MSW landfills shows an increase in temperature with depth below the cover, a peak value near the center of the waste mass, and a decrease in temperature to a value at the base of the cell that is greater than that at the cover (Yeşiller et al. 2005, 2015; Hanson et al. 2010; Jafari et al. 2017). The nonlinearity of the temperature profile diminishes over time, approaching a more linear relationship with depth for older wastes (Yeşiller et al. 2015).

Since the temperatures inside MSW landfills can reach consistently higher and more stable values than their surrounding environment, demonstration projects have been performed to evaluate the feasibility of using landfills as a source of thermal energy. Grillo (2014) installed horizontal heat exchangers on a landfill base liner in New Hampshire and used the extracted energy to heat a maintenance garage and melt snow and ice. Comparing the cost of the system with the heating savings, the author estimated a payback period of 7 years. Faitli et al. (2015a) installed horizontal "slinky"-loop and serpentine-loop heat exchangers and vertical concrete heat exchangers embedded in an MSW landfill in Hungary. Although they reported average heat transfer rates ranging from approximately 770 to 1152 W for the 16 m-long vertical heat exchangers, they did not investigate in-situ thermal properties or report on the performance of the horizontal heat exchangers. Yeşiller et al. (2016) installed a series of vertical heat exchangers in an MSW landfill in California and performed a periodic heat extraction experiment where a fixed volume of water in equilibrium with the outside air temperature was circulated through the closed-loop heat exchangers once a week over the course of a year. They observed a slight decrease in waste temperature over the testing period, but because the heat transfer rate was not quantified it is not possible to evaluate the thermal properties of the waste from their results. Shi et al. (2018) also conducted heat extraction experiments in an MSW landfill in China using 20 m-long horizontal heat exchangers. Heat was extracted in three different stages that lasted from 10 to 17 days and happened within the first 14 months after the placement of the waste in the cell. The authors discussed the temperature variation due to biodegradation and heat extraction, but these results were not used to estimate the thermal conductivity of the waste. Instead, the values of thermal conductivity reported in their study (0.35 to 0.45 W/m°C) were estimated based on the void ratio and water content of the MSW at that landfill.

One of the main waste thermal properties required for the design of a geothermal heat extraction system in an MSW landfill is the thermal conductivity. Yeşiller et al. (2015) reviewed results from laboratory-scale thermal conductivity experiments and found that the thermal conductivity of MSW ranged from 0.044 to 1.5 W/m°C depending on the composition, density, and degree of saturation of the studied material. Faitli et al. (2015b) developed an experimental device to estimate MSW thermal conductivity in which a waste sample is placed in a steel box and compressed by a moveable lid. The vertical compression force is maintained during the test and heat is applied to the waste through resistance heating wires. The device is equipped with temperature and heat flux sensors on the lid and bottom of the box, and the thermal conductivity of the waste is estimated based on the heat flux observed at equilibrium and on the temperature gradient between the lid and bottom of the box. They reported MSW thermal conductivities ranging from 0.24 to 1.15 W/m°C. Hanson et al. (2000) used a needle probe apparatus to measure the thermal conductivity of MSW specimens ranging from 0.01 to 0.7 W/m°C. However, the authors noted that the thermal conductivity measured using the needle probe method may lead to low values in heterogeneous MSW as the positioning of the needle in a specimen may be strongly affected by the presence of air-filled voids. The heterogeneity of the material, along with the wide range of values reported in literature, and the major effect the thermal conductivity has on heat extraction systems emphasize the need for in-situ thermal property characterization.

MATERIALS AND METHODS

Landfill Location and Waste Characterization

A full-scale instrumented geothermal heat extraction system was installed during construction of a new cell at an MSW landfill in Santee, San Diego County, California. The climate in the region is warm and dry, with an average high temperature of 25.9 °C and low of 11.8 °C, and average annual precipitation of 224 mm, with most rainfall occurring during winter (historical series data obtained from the nearby El Cajon, CA weather station). A plan view schematic of the MSW cell is shown in Figure 1(a). The system was installed between the months of August and October of 2016, which coincides with the dry season of the region. During the three month-long construction period, the total precipitation in the landfill was of 16.7 mm. The MSW placed in this cell was not characterized in terms of gravimetric or volumetric composition but is assumed to be typical of the residual waste stream for disposal reported by the City of San Diego (2014). After placement, the waste was compacted to reach an average total unit weight of 8.7 kN/m^3. Due to the dry conditions during the study period and the fact that negligible leachate was collected from the sump, the leachate level is assumed to be below the allowed maximum value of 300 mm above the liner system set by U.S. EPA design criteria for MSW landfills (U.S. EPA 1993).

Instrumentation and Heat Exchanger Layout

The geothermal heat exchanger pipes were placed horizontally with a serpentine configuration in three different elevations of the MSW cell, with a length of 36.5 m inside the waste, as shown in Figure 1(b). The horizontal configuration was chosen as a less expensive alternative when compared to vertical heat exchangers, which require drilling for installation (Coccia et al. 2013; Florides and Kalogirou 2007). Placement of horizontal pipes is simpler and can be integrated with placement of waste in the cell, minimizing interference with landfill operations. The first level of the system, or Layer 1, was placed directly above the base liner and Layers 2 and 3 were placed 6 m and 12 m above the base liner, respectively. This vertical spacing corresponds to one lift of waste, so Layers 2 and 3 were installed in the time interval between the placement of two lifts. The heat exchangers used are high density polyethylene (HDPE) pipes with internal diameter of 25 mm.

Six thermistor strings (Model 3810 from Geokon, Inc. of Lebanon, NH), each containing four thermistors over a single 45 m-cable, were installed horizontally during placement of the waste. The thermistors have an accuracy of ±0.5 °C. The spacing between each thermistor along the string was approximately 15 m, with the first one positioned 1.5 m from the waste slope, as shown in the longitudinal profiles of the waste cell in Figure 1(b). Layers 1 and 3 were instrumented with one thermistor string each, while Layer 2 was more heavily instrumented with four thermistor strings to obtain a more detailed profile of temperature around the heat exchangers, as shown in the perpendicular profile in Figure 1(c). While the sensors were placed 2 m from the heat exchanger pipes in Layer 1 and 3, in Layer 2 they were positioned in a way to provide a horizontal profile of temperatures as a function of time and distance from the pipes. The first thermistor strings in each layer are referred to as String 1A, 2A, and 3A and were each placed 2 m away from the outermost segment of the heat exchanger pipe. In Layer 2, String 2B was placed 1 m from the outermost heat exchanger segment, String 2C was attached to the outermost heat exchanger segment and String 2D was placed between the first out-and-back segments of the serpentine heat exchanger (1 m from each). One additional thermistor with the same accuracy was installed in the data logger to measure the air temperature during the experiment.

The serpentine configuration of the geothermal heat exchanger pipes is shown in Figure 1(d). The pipes were connected in a closed loop manner, with a total length of 310 m of heat exchanger pipe in each layer. A serpentine rather than slinky arrangement was chosen as the latter is generally used to fit more pipes into a given area when the space for installation is limited (e.g., Florides and Kalogirou 2007), which was not an issue in this study. Further, installation of a serpentine system is easier than a slinky system and the calculations of the length of heat exchanger pipe required to meet a given heat extraction demand are simpler. The overlap of pipes in a slinky configuration may also result in stress distribution issues under the high vertical stresses expected in landfill cells. The spacing between the serpentine segments of pipe in each heat exchanger was selected to be 2 m based on ease of installation for this testing program, but this dimension will change depending on the goals of the heat extraction system. For example, a system to control the temperature at a given elevation may have closer spacing between the serpentine segments to encourage overlapping effects, while a system to exchange heat will have a larger spacing to minimize overlapping effects.

Pictures of the installation process are shown sequentially in Figure 2. A photograph taken facing north in Figure 2(a) shows the serpentine configuration of the heat exchangers along with the direction of heat exchanger fluid circulation. In Figure 2(b), a photograph taken facing south shows the position of the four thermistor strings of Layer 2. After the pipes were properly positioned, they were filled with water and were pressurized to 300 kPa to minimize their likelihood of being compressed under the vertical load to be applied by the waste. Next, the sensors and heat exchangers were covered with 150 mm of soil to prevent puncturing by the waste components, as shown in Figure 2(c). A picture of the final configuration of the system, one year after the beginning of the installation, is shown in Figure 2(d). The position of the three layers of geothermal heat exchangers is indicated, as well as the data acquisition system (DAQ) and the chiller and generator used during the heat extraction. Three lifts of waste of 6 m each were placed atop Layer 3, with a total of 30 m of waste in the cell. The lengths of pipe connecting each heat exchanger to the manifold outside the MSW cell were insulated with fiberglass batting to minimize transfer of heat between the fluid and the surrounding air.

In addition to the thermistors installed within the waste and in the datalogger, six pipe plug thermistors (model TH44004 from Omega Engineering, with a resolution of ±0.2°C) were connected to the entrance and exit of each pipe to measure the temperature of the water entering and exiting each heat exchanger. Further, a flowmeter (model SM7601 from IFM Electronic gmbh, with a resolution of 6.309×10^{-5} m^3/s) was connected to each pipe. The fluid temperatures and flow rates can be used together to monitor the heat transfer rate in each heat exchanger, as will be described later. A schematic of the manifold setup is shown in Figure 1(d). The pipes in all three layers were connected so that water would circulate through a water tank and a chiller (i.e., a heat pump), which cooled the water prior to its return to the waste cell through three separate pipes. The mobile industrial chiller used in this study (model SQ2A1004 from Carrier) has a capacity of 10 thermal tons (35 kW) and was powered using a mobile diesel generator.

Testing Stages

The field experiments were conducted in two stages: (i) monitoring the self-heating of the waste during a 13-month period prior to heat extraction, and (ii) a 17-day heat extraction thermal response test (TRT) performed simultaneously on all three heat exchangers. During the first stage, waste temperatures were measured every 15 minutes which permitted evaluating the evolution of temperatures over time to characterize peak temperatures and the distribution in temperature with elevation. After the waste temperatures stabilized, the heat extraction TRT was performed using an approach consistent with that proposed by Mogensen (1983). The test involved circulation of a heat exchanger fluid (water) from the chiller through the closed-loop heat exchangers at a constant volumetric flow rate while tracking the changes in entering and exiting fluid temperatures. The chiller was connected in series with a 3000 L water tank to act as a buffer as the chiller can only operate under a certain maximum heat exchanger fluid temperature difference that depends on its capacity (10 thermal tons), as shown in Figure 1(d). At the beginning of the test, the hot water exiting the heat exchangers mixed with the cooler water in the tank so that the temperature of the fluid drawn into the chiller was closer to its set point. The entering and exiting water temperatures were measured in the manifold before entering and exiting the waste, as shown in Figure 1(d), so the mixing in the water tank did not affect the TRT results.

In this second stage of the field experiment, heat was extracted from the three layers for 405 hours (approximately 17 days) without interruption. Although a TRT is typically performed for only 2-3 days, the heat extraction TRT was performed for a longer duration in this study to track the evolution in waste temperature surrounding the heat exchangers and permit additional analysis of the waste thermal properties. The target set point temperature for water entering the waste was 12 °C, but due to diurnal air temperature fluctuations this value oscillated daily. The total volumetric flow rate supplied by the chiller was 8.5×10^{-4} m^3/s (0.85 L/s), which was balanced through each layer by adjusting ball valves in a pipe distribution manifold. The averaged volumetric flow rates through the heat exchangers in Layers 1, 2 and 3 were 3.2×10^{-4} m^3/s (0.32 L/s), 2.1×10^{-4} m^3/s (0.21 L/s) and 3.2×10^{-4} m^3/s (0.32 L/s), respectively. These flow rates were sufficient to maintain turbulent flow within the 25-mm diameter heat exchanger pipes (i.e., Reynold’s numbers of 20101, 13191 and 20101 for Layers 1, 2 and 3, respectively). Although the volumetric flow rate in Layer 2 was initially the same as the other two layers, due to the iterative process of adjusting the valves to balance the flow through the three layers it changed slightly over the first hours of operation to a lower value. The authors chose not to adjust it after it was set to avoid disruptions in the results, and all three flow rates remained relatively constant during the test duration. During the heat extraction, the temperatures of the fluid and MSW were recorded every 2 minutes and the volumetric flow rates were recorded every 1 minute. After concluding the test, fluid circulation was stopped, and the geothermal heat exchanger pipes were disconnected from the chiller and water tank, ending the second stage of the field experiment.

RESULTS

MSW Self-Heating

Temperature readings from String A in each layer are presented in Figures 3(a), 3(b) and 3(c) for the initial 13-month test period following waste placement. The air temperature is also shown for reference. The results from other thermistor strings in Layer 2 were similar to String 2A during the self-heating monitoring period. The gap in data observed in these figures was due to a problem with the data logger battery, but the trend in all datasets is still clear. A rapid increase in temperature was observed during the first month followed by a slower increase, which suggests a higher rate of heat generation due to aerobic decomposition in the first few weeks followed by a slower heat generation rate as the decomposition process became anaerobic, consistent with observations by Yeşiller et al. (2015). The maximum temperatures registered were 32°C for Layer 1 and 52 °C for Layers 2 and 3, which are within the values reported in the literature for other MSW landfills, which range between 23 °C and 60 °C (Rees 1980a; Lefebvre et al. 2000; Yeşiller et al. 2005; Bouazza et al. 2011; Shariatmadari et al. 2011; Faitly et al. 2015a). These data, especially in Layers 2 and 3, not only confirm the potential for heat extraction in MSW landfills but also show that the heat extraction process can start within a relatively short time (approximately 1 year) after waste placement. The temperatures in Layers 2 and 3 also show that there is potential to extract heat from MSW landfills even if the goal is only to maintain temperatures between 35 °C and 40 °C to optimize the methane generation due to the activity of mesophilic bacteria (Pfeffer 1974; Rees 1980a).

The sharp drop in temperature observed for the sensors at 1.5 m from the slope face occurred when strong winter rains eroded the side slope of the cell, resulting in cracks which reduced the waste cover overlying the outermost sensors. Due to these cracks, it is not possible to know how the air temperature influenced the readings in those sensors. However, it is clear from the results showed that the sensors placed 16.8 m from the slope do not show further seasonal variation in temperatures. Rees (1980b) observed that the minimum depth necessary to avoid seasonal fluctuations in temperature was 3.5 m below the surface, while Yeşiller et al. (2005) observed that the minimum depth and horizontal distance from external slopes necessary to avoid seasonal fluctuations were 7 m and 20 m, respectively. These distances depend on the temperature gradient induced by the surface temperature as well as the characteristics of the cover system.

Vertical profiles of the cell temperatures at the end of the self-heating monitoring period are shown in Figure 3(d). The profiles indicate that the central part of the landfill holds the highest temperatures, while the sensors in Layer 1, located at the base liner of the cell, present the lowest temperatures due to the lower temperature of the underlying subsurface. Since Layer 3 is not at the surface of the cell and is covered by approximately 18 m of waste, the temperatures shown in Figure 3(d) are consistent with waste temperature distributions with depth described in the literature (e.g., Yeşiller et al. 2005, 2015; Hanson et al. 2010; Jafari et al. 2017).

Heat Extraction Thermal Response Test

The results of the TRT in terms of volumetric flow rate and temperature of water entering and exiting the heat exchangers on each Layers 1, 2, and 3 are shown in Figures 4(a), 4(b) and 4(c), respectively. The evolution of fluid temperatures was similar for all layers, with each starting the test with a drop before tending to a stable average value. The influence of daily air temperature fluctuations is clear, but as will be shown later, it is not expected to affect the test results. After the first few hours of heat extraction, the difference between entering and exiting fluid temperatures in each layer (i.e., $T_{in} - T_{out}$) was nearly constant and was approximately -6°C for Layer 1, -13°C for Layer 2 and -11°C for Layer 3. The results in Figures 4(a), 4(b) and 4(c) can be synthesized to calculate the heat transfer rate for the three heat exchangers, as follows:

$$\dot{Q} = c.\rho.\dot{v}.(T_{in} - T_{out}) \quad (1)$$

where $\dot{Q}$ is the heat transfer rate, c is the specific heat capacity of the fluid, ρ is the fluid density, $\dot{v}$ is the volumetric flow rate, and T_{in} and T_{out} are the temperatures of the fluid entering and exiting the heat exchanger loop, respectively. The heat transfer rates during the test for the heat exchangers in each layer are shown in Figure 4(d). Although all three heat transfer rates tend toward stable values, the heat transfer rate for Layer 1 showed an increasing trend while the heat transfer rates for Layers 2 and 3 showed a decreasing trend. This difference can be explained by the waste temperature at each layer before the start of the heat extraction. While the waste in Layers 2 and 3 was at a temperature of 52°C, the waste in Layer 1 was at 32°C, which is closer to the entering fluid temperature at the beginning of the test. As the heat transfer rate is proportional to the difference in entering and exiting fluid temperatures, the heat transfer rate at the beginning of heat extraction is lower for Layer 1, increasing as the entering fluid temperature drops. Daily fluctuations are observed due to the influence of the ambient air temperatures on the water tank, but the heat transfer rates tended to stable average values over time. The average heat transfer rates calculated were -8.1 kW in Layer 1, -11.8 kW in Layer 2 and -14.8 kW in Layer 3, with the negative sign indicating that heat was being extracted from the waste. The average heat transfer rates per length of pipe were -26 W/m for Layer 1, -38 W/m for Layer 2 and -48 W/m for Layer 3. During the 405 hours of the experiment, 50.7 GJ of heat were extracted from the MSW cell, with 11.9 GJ extracted from Layer 1, 17.2 GJ extracted from Layer 2, and 21.6 GJ extracted from Layer 3.

The difference in heat transfer rates observed in the three layers can be explained by analyzing Equation (1). For all layers, the values of specific heat capacity and density of the fluid are the same, so the difference in the heat transfer rates calculated is due to variations of the volumetric flow rate between each layer, and differences between entering and exiting fluid temperatures (ΔT). For layers 1 and 3, the volumetric flow rate is the same, but ΔT is larger for layer 3, which results in a higher value of heat transfer rate. Layer 2, however, presented the lowest volumetric flow rate. But although the volumetric flow rate is directly proportional to the heat transfer rate, a slower flow rate increases the residence time of the fluid within the pipes, which consequently increases the time available for heat transfer. This helps explain why the difference in entering and exiting fluid temperatures for Layer 2 was slightly higher than that for Layer 3, even though the waste at both elevations was at the same temperature before the heat extraction. It also explains why the heat exchanger in Layer 2, although with the lowest volumetric flow rate, still showed an intermediate value of heat transfer rate and total heat extracted when compared with the other two layers.

As mentioned previously, the heat extraction TRT was performed for a longer duration than typical TRTs for geothermal heat exchangers to ensure changes in temperature in a larger area surrounding the heat exchangers. Time series of MSW temperatures during the TRT for Layer 2 are shown in Figure 5. Because String 2A is 2 m from the outermost heat exchanger segment, the temperatures at this location shown in Figure 5(a) decreased only slightly during the heat extraction test, with decreases of 0.7, 1.1 and 1.0 °C for the sensors positioned 1.5 m, 16.8 m and 32.0 m from the slope face, respectively. Similar small decreases in temperature were measured for Strings 1A and 3A. For the sensors positioned 47.2 m from the slope face, no meaningful change in temperature was observed in any layer. Different from the results for String 2A, greater changes in temperatures were observed at some locations on Strings 2B, 2C and 2D in Layer 2, as observed in Figures 5(b), 5(c), and 5(d), respectively. A sharp decrease in temperature was measured by sensors on String 2C as they were attached to the outermost heat exchanger segment, with the sensor at 32.0 m from the slope presenting a drop of nearly 28°C. Decreases in temperature were also measured by sensors on Strings 2B and 2D, but although both strings were equally distant (1 m) from the first segment of heat exchanger, the sensors on String 2D were also influenced by an inner segment of heat exchanger, located 1m from this string, experiencing a superposition of effects and consequently a more accentuated drop in temperature when compared to String 2B. For example, after the 405 hours of test, for the sensors at 32.0 m from the slope the decrease in temperature was 4.6 °C for String 2B, while for String 2D the drop was 9.2 °C, twice the value observed for String 2B.

Horizontal temperature profiles at the locations of 16.8 m and 32.0m from the slope face on Layer 2 are shown in Figures 6(a) and 6(b), respectively. The profile at t = 0 represents the initial conditions of the test. Before the start of the heat extraction test analyzed in this work, three short simplified tests had to be carried out to calibrate the chiller, which reduced the temperatures around String C for t = 0. However, since the drop in temperature in this string occurs rapidly at the beginning of the heat extraction, as observed in Figure 5(c), and the data used for the estimate of the thermal conductivity is for later hours of test, as explained in the next section, it is assumed that this initial variation in temperature does not affect the interpretation of data. The profiles at t = 405 hours in Figures 6(a) and 6(b) represent the final conditions of the test, with the zone of influence of the heat exchanger in the surrounding waste.

ESTIMATION OF IN-SITU EFFECTIVE THERMAL CONDUCTIVITY

Although there are several analytical methods available to estimate the effective thermal conductivity of a geothermal heat exchanger embedded in the subsurface, there is no analytical model specifically developed for serpentine heat exchangers. However, if the segments of the serpentine heat exchanger are placed far enough that they do not interact significantly during the heat extraction, the serpentine can be assumed to be a line source, even though it is not straight. Further, if the diameter of the heat exchanger is small, an infinite line source analysis can be used to determine the thermal conductivity of the material.

The solution of the differential equation for heat conduction in solids for an infinite linear heat source presented by Ingersoll and Plass (1948) and Carslaw and Jaeger (1959) is a common approach to interpret the results from a TRT and estimate the thermal conductivity of soils and rocks (e.g., Mogensen 1983; Gehlin and Hellstrom 2003; Sanner et al. 2005, 2008; Raymond et al. 2011; Stauffer et al. 2013; Murphy et al. 2014). The infinite line source analysis assumes a constant heat transfer rate per length of pipe $\dot{Q}_L$ and an infinite length of heat exchanger embedded in the subsurface at an initial temperature T_0, and it provides the temperature T of the medium at a radial distance r from the center line of the line heat source at a time t, as follows:

$$T = T_0 + \frac{\dot{Q}_L}{4\pi\lambda}\int_{\frac{r^2}{4\alpha t}}^{\infty}\frac{e^{-\beta}}{\beta}d\beta \tag{2}$$

where λ and α are the thermal conductivity and thermal diffusivity of the material surrounding the line heat source, respectively, and β is a variable of integration. This analysis assumes the heat transfer occurs solely due to conduction, neglecting the effects of convection. It also neglects the effects of heat generation within the conductive material, which might be unsuitable for applications with MSW. However, for the system presented in this study, the temperatures in the MSW had been nearly constant for months before the heat extraction, and there is no oxygen being introduced in the cell – which could potentially increase the heat generation rate. Therefore, it is assumed that the heat generation rate was low enough, so that its influence on waste temperature during the period of heat extraction can be neglected. For $t > 4r^2/\alpha$ (Mogensen 1983), the exponential integral in Equation (2) can be simplified to obtain the following equation (Carslaw and Jaeger 1959):

$$T - T_0 = \frac{\dot{Q}_L}{4\pi\lambda}\left(\ln t + \ln\frac{4\alpha}{r^2} - \gamma\right) \quad (3)$$

where γ is Euler's constant. This solution is suitable to analyze TRT results as the fluid temperatures are representative of the heat source and the duration of TRTs is typically several times longer than the minimum time required for this approximation to be valid. For example, for a 25 mm-diameter pipe in a medium with $\alpha = 3.0\times10^{-7}$ m^2/s, the minimum time required for this approximation to be valid at the wall of the pipe is 35 minutes. Regarding the duration of the TRT, ASHRAE (2002) recommends 36 to 48 hours of test to ensure enough time for the data to converge. Sanner et al. (2005) recommends a minimum of 48 hours and Signorelli et al. (2007) suggests a test duration of 50 hours to obtain stable results.

To apply Equation (3) to interpret TRT results, a value of temperature T^* is plotted versus the natural logarithm of time t (in seconds, to be consistent with the units used in this work) and the slope of the linear portion of the curve obtained is used to calculate the thermal conductivity λ of the heat exchanger system, as follows:

$$\lambda = \frac{\dot{Q}}{4\pi L}\left[\frac{d(T^*)}{d(\ln t)}\right]^{-1} \quad (4)$$

where L is the length of the pipe through which there is exchange of heat and $\dot{Q}$ is the heat transfer rate, calculated using Equation (1). For heat exchangers with a small ratio r/L, the source of heat can be approximated by an infinite line and $\dot{Q}_L$ is equal to $\dot{Q}/L$ (in this study, $r/L = 4.0\times10^{-5}$). For the value of the temperature T^*, different approaches have been proposed in the literature. The approach of Mogensen (1983) and ASTM (2014), often referred to as the transient probe method, defines T^* as the difference between the fluid temperature exiting the heat exchanger measured at time t and the fluid temperature exiting the heat exchanger at the beginning of the test (i.e., the difference fluid temperature, ΔT, in time). The most common approach used in TRT analyses is referred to as the average fluid temperature method, and defines T^* as the average of the temperatures of the fluid entering and exiting the heat exchanger (i.e., the average fluid temperature, T_{ave}) (ASHRAE 2002; Gehlin and Spitler 2002; Sanner et al. 2005; Murphy et al. 2014). Although the transient probe method allows the convenience of estimating the thermal conductivity of the system with only one temperature sensor, the use of the two sensors in the average fluid method enables the observer to account for changes in heat transfer rate during the TRT. For this study, both approaches were considered. It is important to highlight that the thermal conductivity determined by the infinite line source analysis as presented in this paper, is an effective thermal conductivity. In other words, it represents a thermal property of the whole heat extraction system, which accounts for the MSW, but also for the heat exchanger pipes, the protective layer of soil, and the circulating fluid.

Examples of the plots of T^* as a function of the logarithm of time for the heat exchanger on Layer 2 are shown in Figures 7(a) and 7(b) for the transient probe method using the exiting fluid temperature, and the average fluid temperature method, respectively. In both plots, an initial nonlinear decrease is observed in the first 20 hours of heat extraction, after which a log-linear decrease is observed. The best-fit linear trends for the period of 20 to 405 hours are shown. The influence of the daily fluctuations in air temperature is clearly observed in the data, but the best-fit lines follow the average slope of the data. These daily fluctuations in air temperature are shown in Figure 8: although they caused noise in the experimental data, the noise was periodic and the average daily temperature did not change significantly over the 17 days of the experiment (i.e., 19.1 ± 1.3 °C). This implies that the daily fluctuations in air temperature did not lead to a bias that affected the slope of the data during heat extraction.

In addition to fitting lines to the data between 20 and 405 hours as shown in Figures 7(a) and 7(b), which are referred to as long-term analyses, lines were also fitted to the data between 20 and 100 hours, which are referred to as short-term analysis. The reason for performing two analyses is to guarantee that overlapping effects between two segments of the serpentine heat exchanger are not occurring. A summary of the estimated values of thermal conductivity using both long-term and short-term analyses is shown in Table 1, and only slight differences between the short-term and long-term analyses are observed. Therefore, it is likely that even after 17 days of heat extraction, the overlapping effect in the segments of the serpentine heat exchanger did not affect the assumption of a line source heat exchanger. Further, the fact that the values remained the same also confirms that for the duration of this heat extraction test, the possible effects of heat generation can be neglected. Table 1 summarizes the results from the transient probe method and the average fluid temperature method, along with the specific sensors used in each analysis. Variations in thermal conductivity of about 10% were observed for the different analysis approaches. The thermal conductivity values in Table 1 are consistent with the upper bound of the MSW thermal conductivity values reported in the literature, which range from 0.01 to 1.5 W/m°C (Hanson et al. 2000; Yeşiller et al. 2015; Faitli et al. 2015b). The variability of two orders of magnitude in the values reported in the literature, which were obtained from laboratory experiments, reinforces the relevance of estimating the thermal conductivity of MSW in-situ. A trend of increasing thermal conductivity is observed with increasing elevation in Figure 9, even when accounting for the spread in values resulting from the use of different methods and time intervals. While it was expected that MSW near the base liner would have a higher thermal conductivity due to accumulation of leachate at the base of the landfill (e.g., Gibbons et al. 2014), this was not reflected in the results for Layer 1. Two main factors might have led to the unexpected trend in thermal conductivity with elevation. First, although the leachate head above the liner was not monitored in this study, the landfill is in a dry climate area and the precipitation in the six months preceding the test was only 5mm (Gillespie Field Airport weather station, El Cajon, CA), suggesting that the waste is relatively dry and might not be saturated above the liner. Second, the thermal response of the heat exchanger on Layer 1 is affected by the thermal characteristics of the base liner materials (e.g., geosynthetics, compacted clay), as the MSW is only above the heat exchanger on Layer 1, but not below it. Although the materials below the liner are all denser than the waste, it is expected that they have lower thermal conductivity. The geosynthetic most predominantly used in base liners is HDPE geomembrane (Rowe and Hoor 2009), which has a thermal conductivity of approximately 0.34 W/m°C (Singh and Bouazza 2013). The thermal conductivity of clays is sensitive to the degree of saturation, with a decrease in thermal conductivity with degree of saturation. Reported values for the thermal conductivity of compacted clay are often below 1.0 W/m°C (Beziat et al. 1988; Rowe and Hoor 2009; Li et al. 2012). Ali et al. (2016) estimated that the effective thermal conductivity of geosynthetic clay liners (GCLs) is between 0.2 W/m°C and 0.7 W/m°C, while Singh and Bouazza (2013) obtained values ranging from 0.16 W/m°C to 1.07 W/m°C, with the lowest values corresponding to drier GCLs and the highest values corresponding to hydrated GCLs. Since the thermal conductivity obtained in this study reflects properties of the whole heat extraction system (i.e. all the materials through which heat is transferred), the half-space formed by the base liner material and subsurface soil may have a strong influence on the thermal conductivity estimated for Layer 1, lowering its final value when in the dry conditions observed. Although not monitored in this study, other variables might affect the trend of thermal properties with elevation. In addition to the effects of waste heterogeneity, it is expected that the thermal properties will vary with elevation due to density variations (e.g., Kavazanjian et al. 1995; Zekkos et al. 2006). The difference in thermal conductivity for the elevations of Layers 2 and 3 may be associated with the difference in testing conditions for the two layers leading to different heat transfer rates, as greater values of $\dot{Q}$ in Equation (4) may lead to greater thermal conductivity values. It is also possible that a greater degree of biodegradation in the upper portion of the landfill led to an increase in density that contributed to the greater thermal conductivity in those regions.

When comparing values of thermal conductivity obtained with the infinite line source analysis, which represent a thermal property of the system (the MSW, the cover soil material, the heat exchanger pipes and the heat exchanger fluid) with values that represent MSW thermal conductivity only, it is reasonable to expect that the system values obtained in this work are lower than the values for MSW exclusively. Specifically, both the heat exchanger pipes and the heat exchanger fluid (water) have lower values of thermal conductivity when compared to MSW, so they would lead to a lower effective thermal conductivity. Nonetheless, as these components are part of a heat exchange system that would be installed in the waste, the effective thermal conductivity is useful in heat exchanger design calculations.

CONCLUSIONS

This study presented the in-situ thermal conductivity of a heat extraction system installed at different elevations in an MSW landfill estimated from a 17-day heat extraction test performed on horizontal, serpentine geothermal heat exchangers. Prior to the heat extraction tests, the evolution in waste temperature was monitored for a period of 13 months until the waste temperature stabilized. The maximum temperatures observed within the waste are in accordance with the presented in literature for MSW. The values of estimated effective thermal conductivity ranged from 0.86 to 1.32 W/m°C, and a trend of increasing thermal conductivity with elevation was observed. These values are consistent with the upper bound of the thermal conductivity values obtained for MSW from laboratory tests reported in the literature, indicating the relevance of determining this variable in-situ. The approach used for installing the geothermal heat exchangers horizontally in a serpentine configuration within the MSW cell is feasible for full-scale applications as it does not require drilling or interruption of the landfill operations, significantly reducing the costs of installation. The approaches used to interpret the in-situ effective thermal conductivity from the heat extraction test may be useful in developing design guidelines for geothermal heat extraction systems in MSW landfills.

Data Availability Statement

All data, models, and code generated or used during the study appear in the submitted article.

ACKNOWLEDGEMENTS

Funding from the Technical Advisory Committee of Geosyntec Consultants is greatly appreciated. The generous support of Republic Services, Inc. in providing a test site and assisting with planning and installation of the heat exchanger system is gratefully acknowledged, along with the help of Gabe Gonzales and Jamie C. Harris with the installation of the system and Jesus C. Torres and Neil Mohr with the implementation planning. The scholarship received by the first author from the Brazilian Federal Agency for Support and Evaluation of Graduate Education - CAPES (Process no. 99999.002164/2015-09) is highly appreciated.

REFERENCES

Ali, M.A., Bouazza, A., Singh, R.M., Gates, W.P., Rowe, R.K. (2016). "Thermal conductivity of geosynthetic clay liners." *Canadian Geotechnical Journal*. 53(9), 1510-1521.

ASHRAE. (2002). “Methods for determining soil and rock formation thermal properties from field tests.” *ASHRAE Research Summary – ASHRAE 1119-TRP*. American Society of Heating, Refrigerating and Air-Conditioning Engineers, 6 p.

ASTM D5334. (2014). *Standard Test Method for Determination of Thermal Conductivity of Soil and Soft Rock by Thermal Needle Probe Procedure*. ASTM Int., West Conshohocken, PA.

Baldwin, T.D., Stinson, J., and Ham, R.K. (1998). “Decomposition of specific materials buried within sanitary landfills.” *J. Environmental Engineering*, 124(12), 1193-1202.

Bareither, C.A., Breitmeyer, R.J, Benson, C.H., Barlaz, M.A., and Edil, T.B. (2012). “Deer track bioreactor experiment: field-scale evaluation of municipal solid waste bioreactor performance. *Journal of Geotechnical and Geoenvironmental Engineering.* 138(6), 658-670.

Barlaz, M.A., Ham, R.K., and Schaefer, D.M. (1990). “Methane production from municipal refuse: A review of enhancement techniques and microbial dynamics.” *CRC Crit. Reviews Environ. Cont.*, 19(6), 557-584.

Beziat, A., Dardaine, M., Gabis, V. (1988), “Effect of compaction pressure and water content on the thermal conductivity of some natural clays.” *Clays and Clay Minerals*. 36(5), 462-466.Bookter, T.J., and Ham, R.K. (1982). “Stabilization of solid waste in landfills.” *J. Environmental Engineering*, 108(6), 1089-1100.

Bouazza, A., Nahlawi, H., Aylward, M. (2011). “In situ temperature monitoring in an organic-waste landfill cell.” *Journal of Geotechnical and Geoenvironmental Engineering*. 137 (12), 1286-1289.

Carslaw, H.S., and Jaeger, J.C. (1959). *Conduction of Heat in Solids*. 2nd Ed., Oxford University Press, Great Britain. 510 p.

Christensen, T.H., Kjeldsen, P., and Stegmann R. (1992) "Effects of landfill management procedures on landfill stabilization and leachate and gas quality." *Landfilling of Waste: Leachate*. Elsevier Applied Science, London, UK.

City of San Diego. (2014). *Waste Characterization Study: 2012-2013.* Accessed from http://bit.ly/2phuTCz in January 2014.

Coccia, C.J.R., Gupta, R., Morris, J., and McCartney, J.S. (2013). "Municipal solid waste landfills as geothermal heat sources". *Renewable and Sustainable Energy Reviews*. 19, 463-474.

Emmi, G., Zarrella, A., Zuanetti, A., and De Carli, M. (2016) "Use of municipal solid waste landfill as heat source of heat pump." *Energy Procedia*, 101, 352-359.

Faitli, J., Erdélyi, A., Kontra, J., Magyar, T., Várfalvi, J., and Murányi, A. (2015a). "Pilot scale decomposition heat extraction and utilization system built into the "Gyál Municipal Solid Waste Landfill"." *Proc. Sardinia 2015: 15th Int. Waste Mgmt. and Landfill Symp.* 12 p.

Faitli, J., Magyar, T., Erdélyi, A., and Murányi, A. (2015b). "Characterization of thermal properties of municipal solid waste landfills." *Waste Management*. 36, 213-221.

Farquhar, G.J., and Rovers, F.A. (1973). "Gas production during refuse decomposition." *Water, Air, and Soil Pollution*. 2(4), 483-495.

Florides, G., and Kalogirou, S. (2007). "Ground heat exchangers – A review of systems, models and applications." *Renewable Energy*. 32, 2461-2478.

Gehlin, S., and Spitler, J. D. (2002). *Thermal Response Test – State of the Art 2001*. IEA ECES Annex 13, International Energy Agency: Energy Conservation through Energy Storage. 34 p.

Gehlin, S.E., and Hellstrom, G. (2003). "Comparison of four models for thermal response test evaluation". *ASHRAE Transactions*, 109, 1-12.

Gibbons, R.D., Morris, J.W.F., Caldwell, M.D., Prucha, C.P., and Staley, B.F. (2014). "Longitudinal data analysis in support of functional stability concepts for leachate management at closed municipal landfills." *Waste Management*. 34(9), 1674-1682,

Grillo, R.J. (2014) "Energy recycling – landfill waste heat generation and recovery". *Current Sustainable Renewable Energy Reports*. 1(4), 150-156.

Hanson, J.L., Edil, T.B., and Yeşiller, N. (2000). "Thermal properties of high water content materials." Edil, T.B., Fox, P.J., Eds. *Geotech. of High Water Cont. Mat*. ASTM STP 1374, 137-151.

Hanson, J.L., Yeşiller, N., and Oettle, N.K. (2010). "Spatial and temporal temperature distributions in municipal solid waste landfills." *Journal of Environmental Engineering*, 136(8), 804-814.

Hao, Z., Sun, M., Ducoste, J.J., Benson, C.H., Luettich, S., Castaldi, M.J., and Barlaz, M.A. (2017). "Heat generation and accumulation in municipal solid waste landfills." *Env. Sci. & Technol*. 51, 12434-12442.

Ingersoll, L.R., and Plass, H.J. (1948). "Theory of the ground pipe heat source for the heat pump." *Heating, Piping & Air Conditioning*. 20(7), 119-122.

Jafari, N.H., Stark, T.D., and Roper, R. (2014a). "Classification and reactivity of aluminum production waste". *Journal of Hazardous, Toxic and Radioactive Waste*. 18(4), 11p.

Jafari, N.H., Stark, T.D., and Rowe, K. (2014b). "Service life of HDPE geomembranes subjected to elevated temperatures." *Journal of Hazardous, Toxic and Radioactive Waste*. 18(1), 16-26.

Jafari, N.H., Stark, T.D., and Thalhamer, T. (2017). "Progression of elevated temperatures in municipal solid waste landfills." *Journal of Geotechnical and Geoenvironmental Eng*. 143(8).

Kavazanjian, E., Jr., Matasovic, N., Bonaparte, R., Schmertmann, G.R. (1995). "Evaluation of MSW properties for seismic analysis." *Geoenvironment 2000*. 2, 1126-1141.Kjeldsen, P.K., Barlaz, M.A., Rooker, A.P, Baun, A., Ledin, A., and Christensen T.H. (2003). "Present and long-term composition of MSW landfill leachate: A review." *Crit. Rev. Environ. Sci. Tech*. 32(4), 297-336.

Lamothe, D., and Edgers, L. (1994). "The effects of environmental parameters on the laboratory compression of refuse." Proc. 17th Int. Madison Waste Conf. Madison, WI. 592–604.

Lefebvre, X., Lanini, S., Houi, D. (2000). "The role of aerobic activity on refuse temperature rise, I. Landfill experimental study." *Waste Management & Research*, 18(5), 444-452.

Li, Y., Wu, C., Xing, X., Yue, M., Shang, Y. (2012). "Testing and Analysis of the Soil Thermal Conductivity in Tropical Desert and Grassland of West Africa." *Proc. 9th International Pipeline Conference*. Calgary, Canada, 9p.Mogensen, P. (1983). "Fluid to duct wall heat transfer in duct system heat storages." *Proc. Int. Conference on Subsurface Heat Storage in Theory and Practice*. Stockholm, 1983, 652-659.

Murphy, K.D., Henry, K.S., and McCartney, J.S. (2014). "Impact of horizontal run-out length on the thermal response of full-scale energy foundations." *Proc. GeoCongress 2014*. ASCE, Reston, VA, 2715-2724.

Pfeffer, J.T. (1974) "Temperature effects on anaerobic fermentation of domestic refuse." *Biotechnology and Bioengineering*. 16(6), 771-787.

Pohland, F.G., and Harper, S.R. (1986). *Critical Review and Summary of Leachate and Gas Production from Landfills*. Report EPA/6002-86/073. Environmental Protection Agency, Cincinnati, USA.

Raymond, J., Therrien, R., Gosselin, L., and Lefebvre, R. (2011) "A review of thermal response test analysis using pumping test concepts." *Ground Water*. 49(6), 932-945.

Rees, J.F. (1980a). “Optimisation of methane production and refuse decomposition in landfills by temperature control.” *Journal of Chemical Technology and Biotechnology*. 30(1), 458-465.

Rees, J.F. (1980b). “The fate of carbon compounds in the landfill disposal of organic matter.” *Journal of Chemical Technology and Biotechnology*. 30(1), 161-175.

Rowe, R.K., Hoor, A. (2009). “Predicted temperatures and service lives of secondary geomembrane landfill liners.” Geosynthetics International. 16(2), 71-82.Sanner, B., Hellstrom, G., Spitler, J., and Gehlin, S. (2005). “Thermal response test – current status and world-wide application.” *Proc. World Geothermal Congress*. Antalya, Turkey, 10 p.

Sanner, B., Mands, E. Sauer, M.K., and Grundmann, E. (2008). “Thermal response test, a routine method to determine thermal ground properties for GSHP design.” *Proc. 9th International IEA Heat Pump Conference*. Zurich, Switzerland, 12 p.

Shariatmadari, N., Mansouri, A., Zarrabi, M. (2011). “Monitoring the Temperature in a Sanitary Landfill in Tehran.” *Proc. Geo-Frontiers 2011*. ASCE, Dallas TX, 1016-1022.

Shi, J., Zhang, T., Zhang, J., Ai, Y., and Zhang, Y. (2018) “Prototype heat exchange and monitoring system at municipal solid waste landfill in China.” *Waste Manag*. 78, 659-668.

Signorelli, S., Bassetti, S., Pahud, D., and Kohl, T. (2007) “Numerical evaluation of thermal response tests.” *Geothermics*. 36, 141-166.

Singh, R.M., Bouazza, A. (2013). “Thermal conductivity of geosynthetics.” *Geotextiles and Geomembranes*. 39, 1-8.Southen, J., and Rowe, R.K. (2005). “Laboratory investigation of geosynthetic clay liner desiccation in a composite liner subjected to thermal gradients.” *Journal of Geotechnical and Geoenvironmental Engineering*. 131(7), 925–35.

Staley, B.F., and Barlaz, M.A. (2009). "Composition of municipal solid waste in the U.S. and implications for carbon sequestration and methane yield." *J. Environmental Engineering*. 135(10), 901-909

Stark, T.D., Martin, J.W., Gerbasi, G.T., Thalhamer, T., and Gortner, R.E. (2012) "Aluminum waste reactions indicators in a municipal solid waste landfill." *Journal of Geotechnical and Geoenvironmental Engineering*. 138(3), 252-261.

Stauffer, F., Bayer, P., Blum, P., Giraldo, N., and Kinzelbach, W. (2013). *Thermal Use of Shallow Groundwater*. Boca Raton: CRC Press. 250 p.

U.S. EPA. (1993). *Criteria for Solid Waste Disposal Facilities: A Guide for Owners/Operators*. EPA/530-SW-91-089, 22 p.

Yeşiller, N., Hanson, J.L., and Liu, W.L. (2005). "Heat generation in municipal solid waste landfills." *Journal of Geotechnical and Geoenvironmental Engineering*. 131(11), 1330-1344.

Yeşiller, N., Hanson, J.L., and Yee, E.H. (2015). "Waste heat generation: a comprehensive review." *Waste Management*. 42, 166-179.

Yeşiller, N., Hanson, J.L., and Kopp, K.B. (2016). "The design and installation of a prototype heat extraction system at a municipal solid waste landfill." *Geo-Chicago 2016: Geotechnics for Sustainable Energy*. ASCE, Reston VA, 311-320.

Young, A. (1992). *Application of Computer Modelling to Landfill Processes*. DoE Report No. CWM 039A/92. Department of Environment (UK).

Zekkos, D., Bray, J.D., Kavazanjian Jr., E., Matasovic, N., Rathje, E.M., Riemer, M.F., Stokoe II, K.H. (2006). "Unit weight of municipal solid waste." *Journal of Geotechnical and Geoenvironmental Engineering*. 132(10), 1250-1261.

TABLE 1: Summary of heat extraction thermal response test (TRT) results.

Method for defining T* in the infinite line source analysis	Temperature sensor(s) used	Thermal conductivity (W/m°C)[1]			Thermal conductivity (W/m°C)[2]		
		Layer 1	Layer 2	Layer 3	Layer 1	Layer 2	Layer 3
Transient probe $T^* = \Delta T$	Exiting fluid temperatures for each layer (T_{out})	0.94	1.12	1.17	0.94	1.03	1.16
Average fluid temperature $T^* = T_{ave}$	Entering and exiting fluid temperatures for each layer (T_{in}, T_{out})	0.86	1.11	1.28	0.89	1.12	1.32

[1]Short-term analysis (20 to 100 hours)
[2]Long-term analysis (20 to 405 hours)

LIST OF FIGURES

Click here to access/download;Figure;Figure 1.tiff

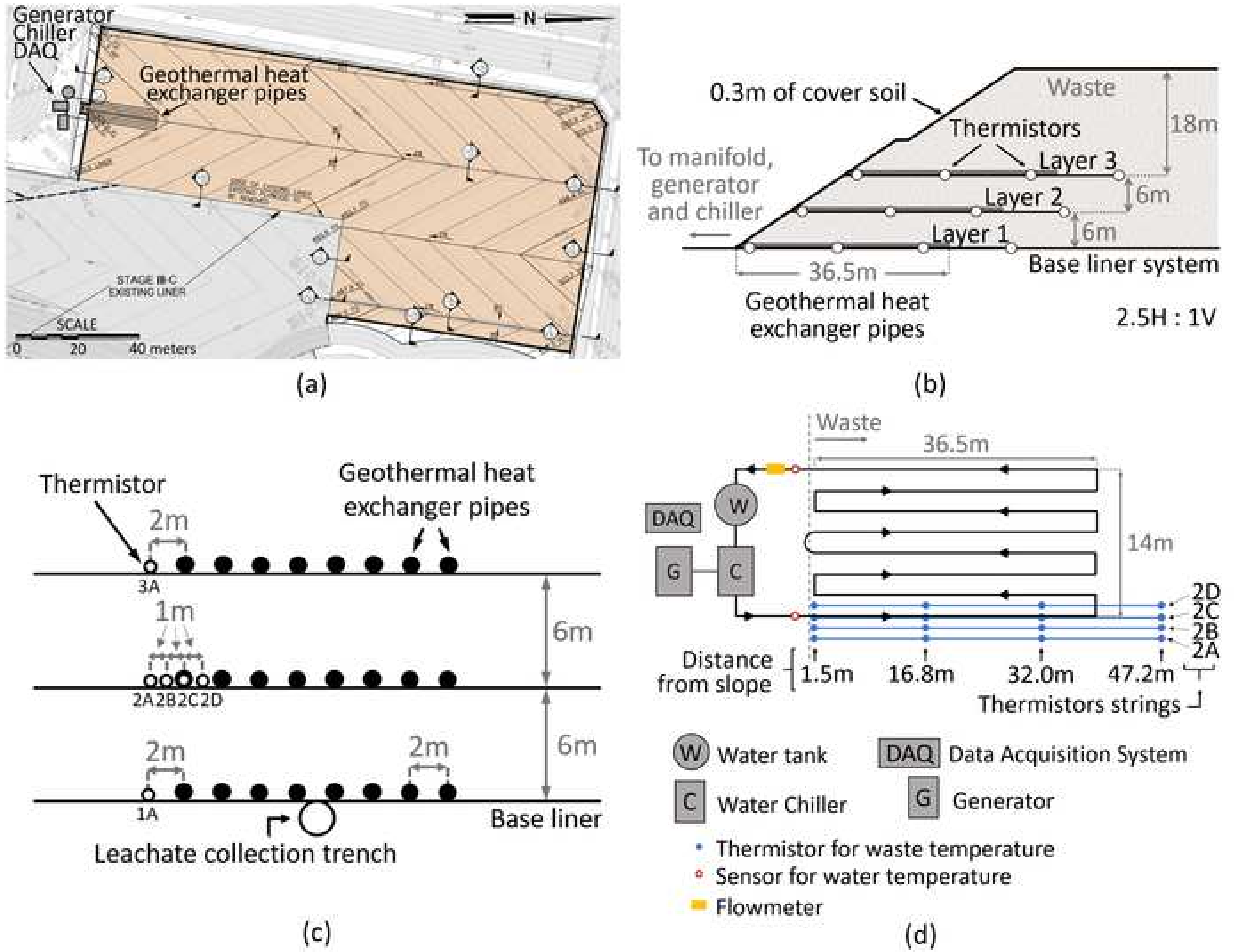

Click here to access/download;Figure;Figure 2.tif

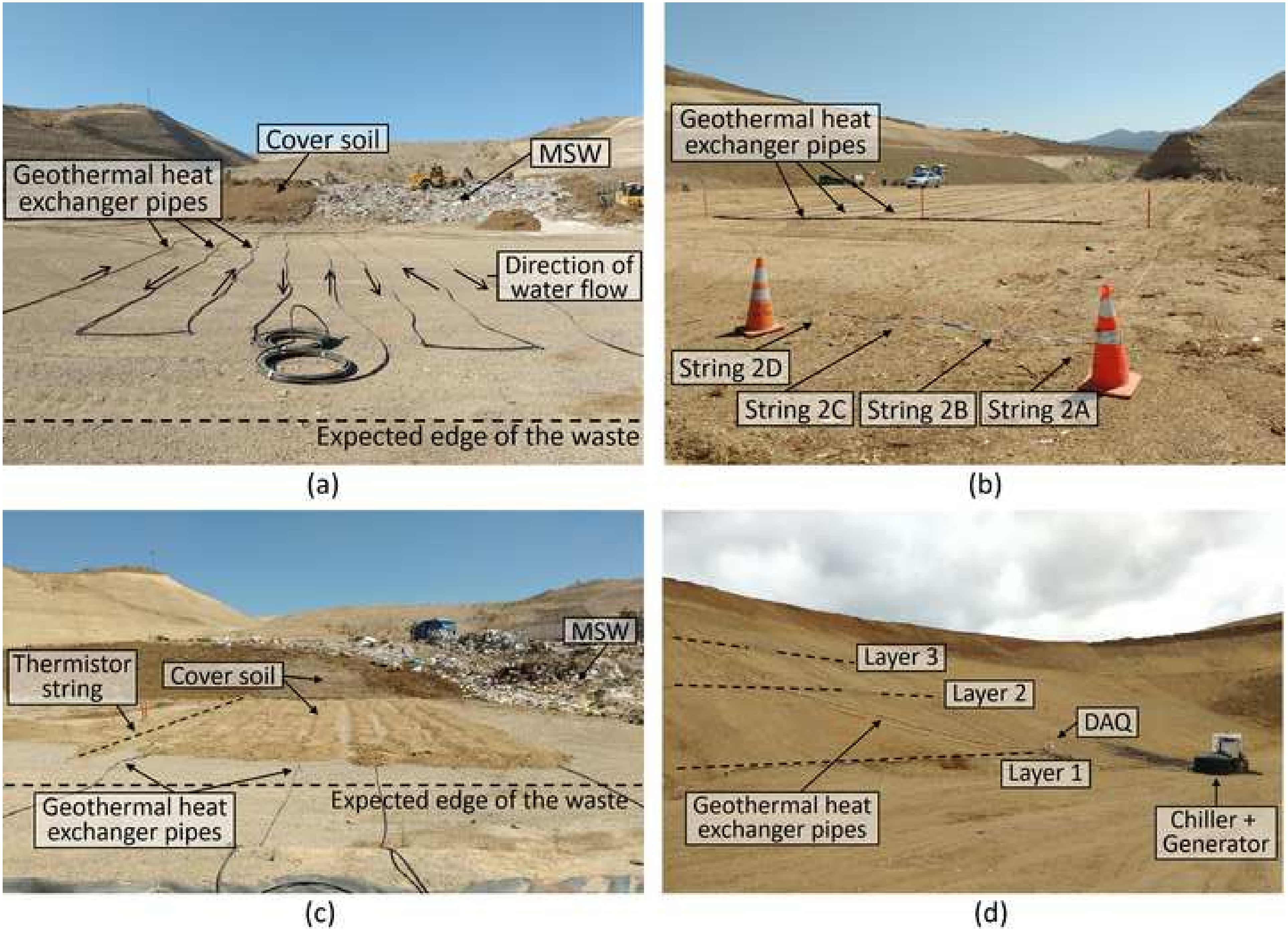

Click here to access/download;Figure;Figure 3.tif

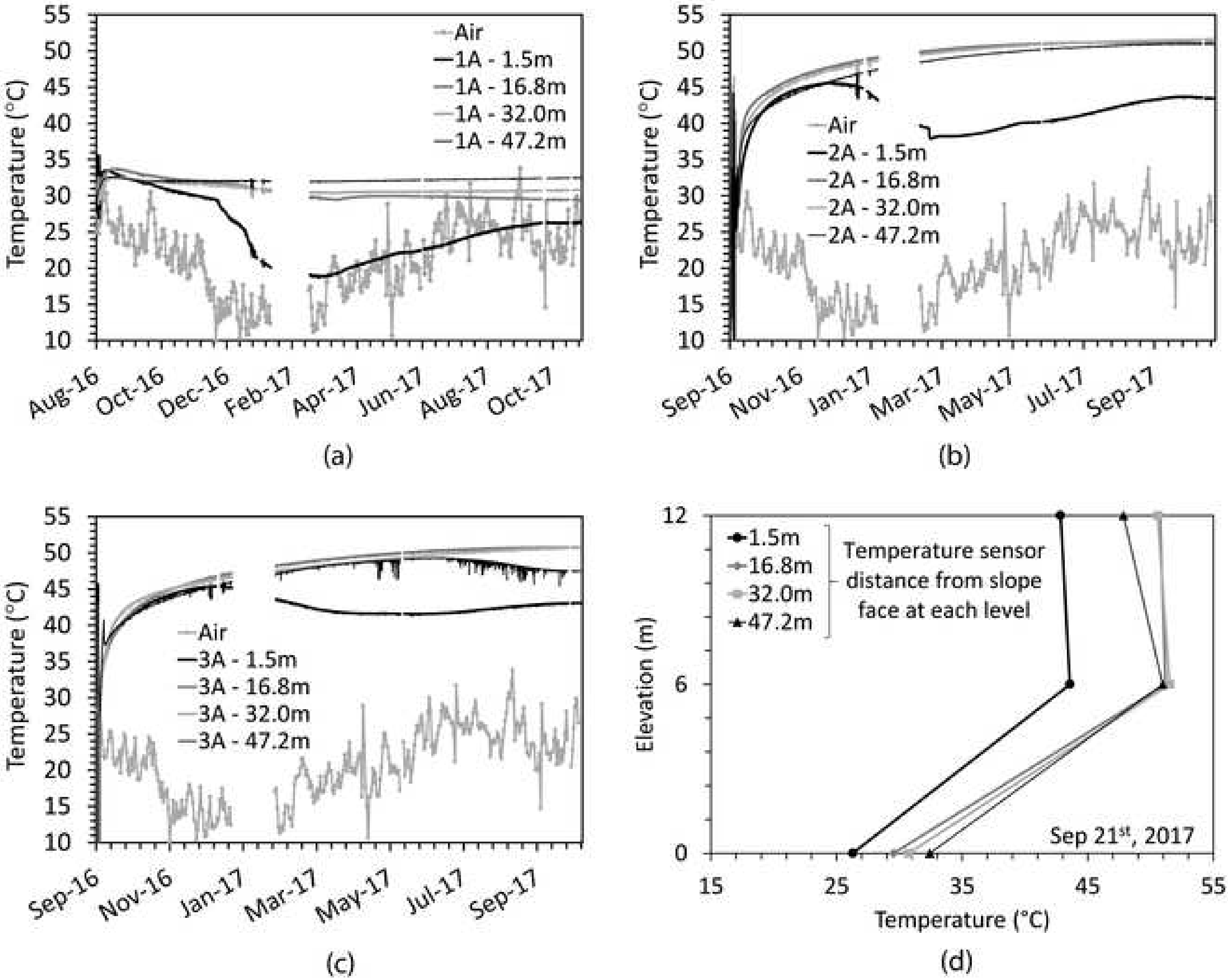

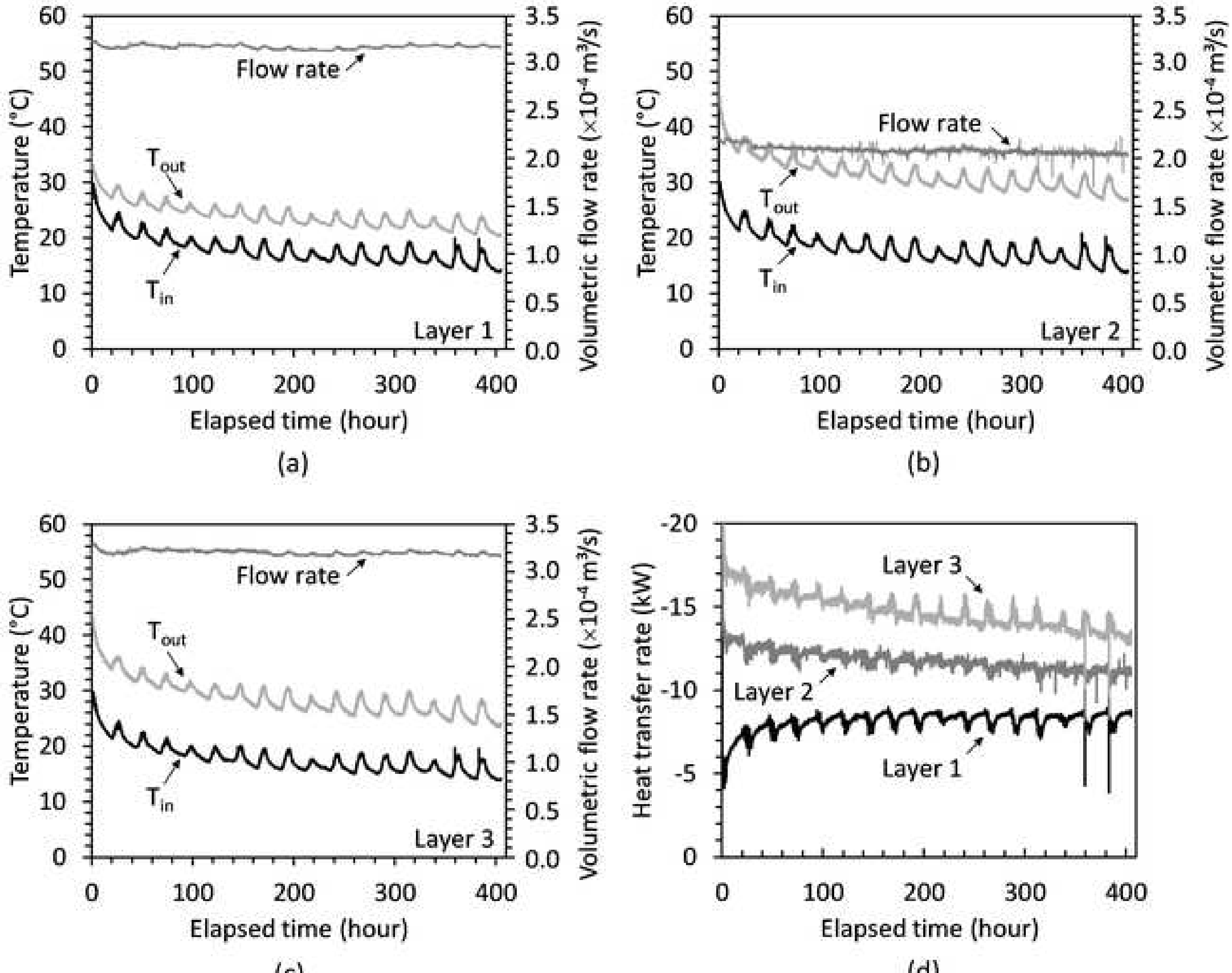
60
50
40
30
20
10
0
Temperature (°C)
3.5
3.0
2.5
2.0
1.5
1.0
0.5
0.0
Volumetric flow rate (×10-4 m3/s)
0
100
200
300
400
Elapsed time (hour)
Flow rate
Tout
Tin
Layer 1
Layer 2
Layer 3
Heat transfer rate (kW)
-20
-15
-10
-5
(a)
(b)
(c)
(d)

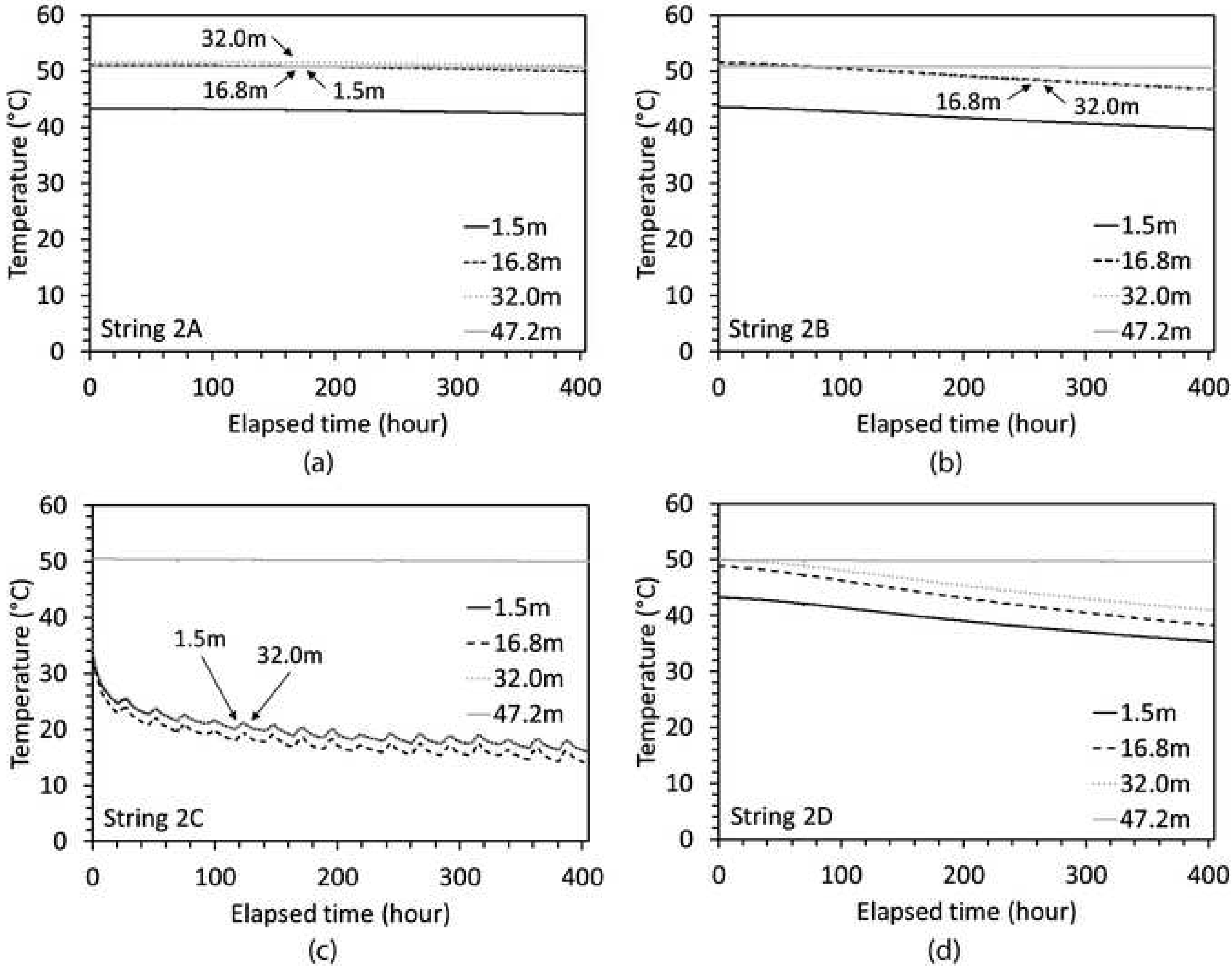
60
50
40
30
20
10
0
Temperature (°C)
32.0m
16.8m
1.5m
—1.5m
---16.8m
32.0m
47.2m
String 2A
0
100
200
300
400
Elapsed time (hour)
(a)
String 2B
16.8m
32.0m
(b)
String 2C
1.5m
32.0m
(c)
String 2D
(d)

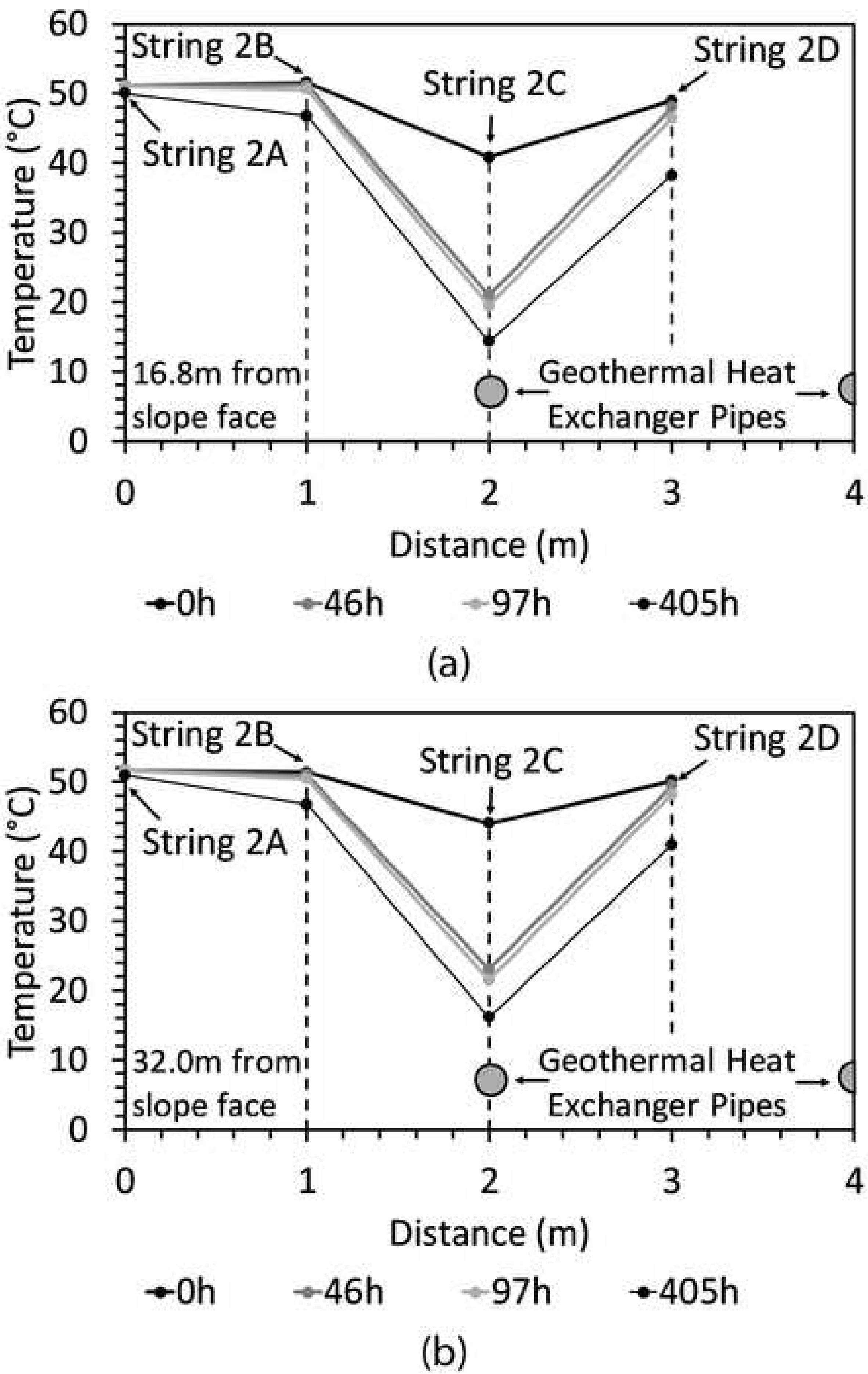

60
50
40
30
20
10
0
Temperature (°C)
String 2B
String 2C
String 2D
String 2A
16.8m from
slope face
Geothermal Heat
Exchanger Pipes
0
1
2
3
4
Distance (m)
0h
46h
97h
405h
(a)
60
50
40
30
20
10
0
Temperature (°C)
String 2B
String 2C
String 2D
String 2A
32.0m from
slope face
Geothermal Heat
Exchanger Pipes
0
1
2
3
4
Distance (m)
0h
46h
97h
405h
(b)

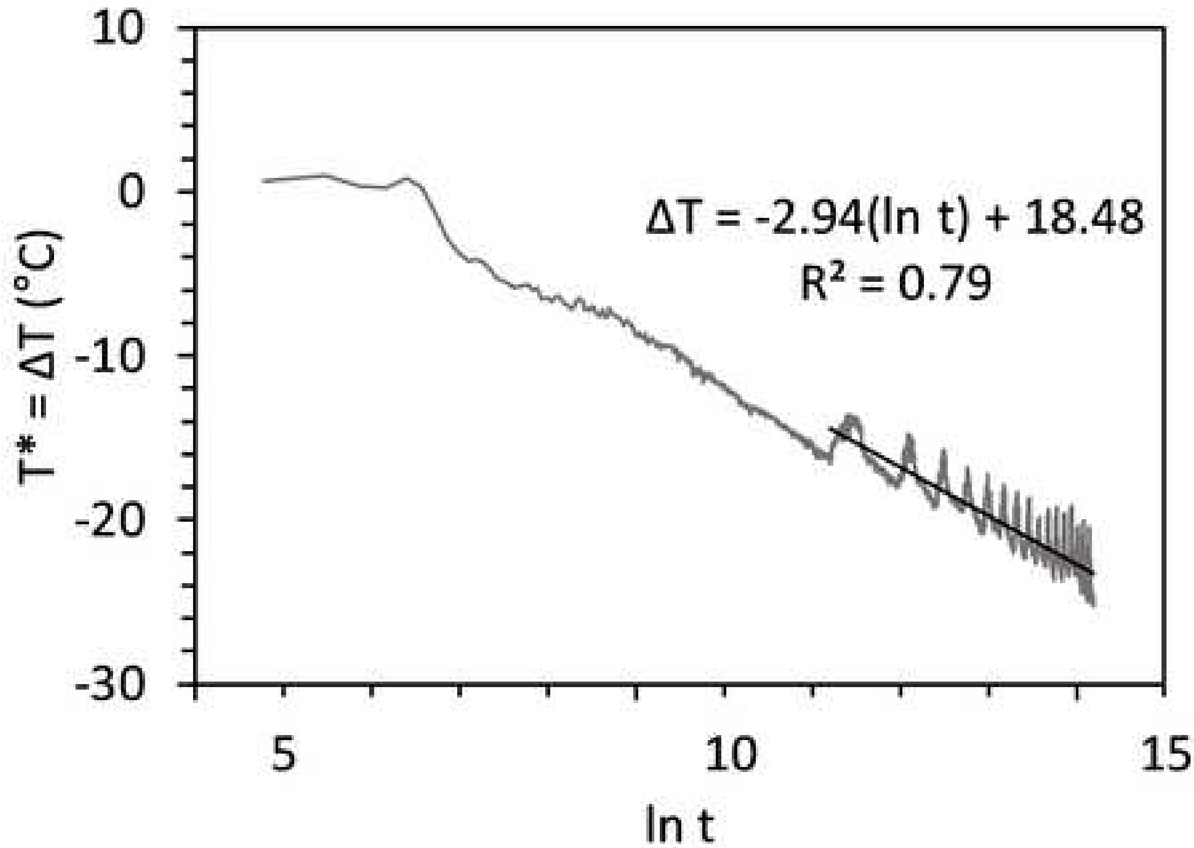

10
0
-10
-20
-30
T* = ΔT (°C)
5
10
15
ln t
ΔT = -2.94(ln t) + 18.48
R² = 0.79

(a)

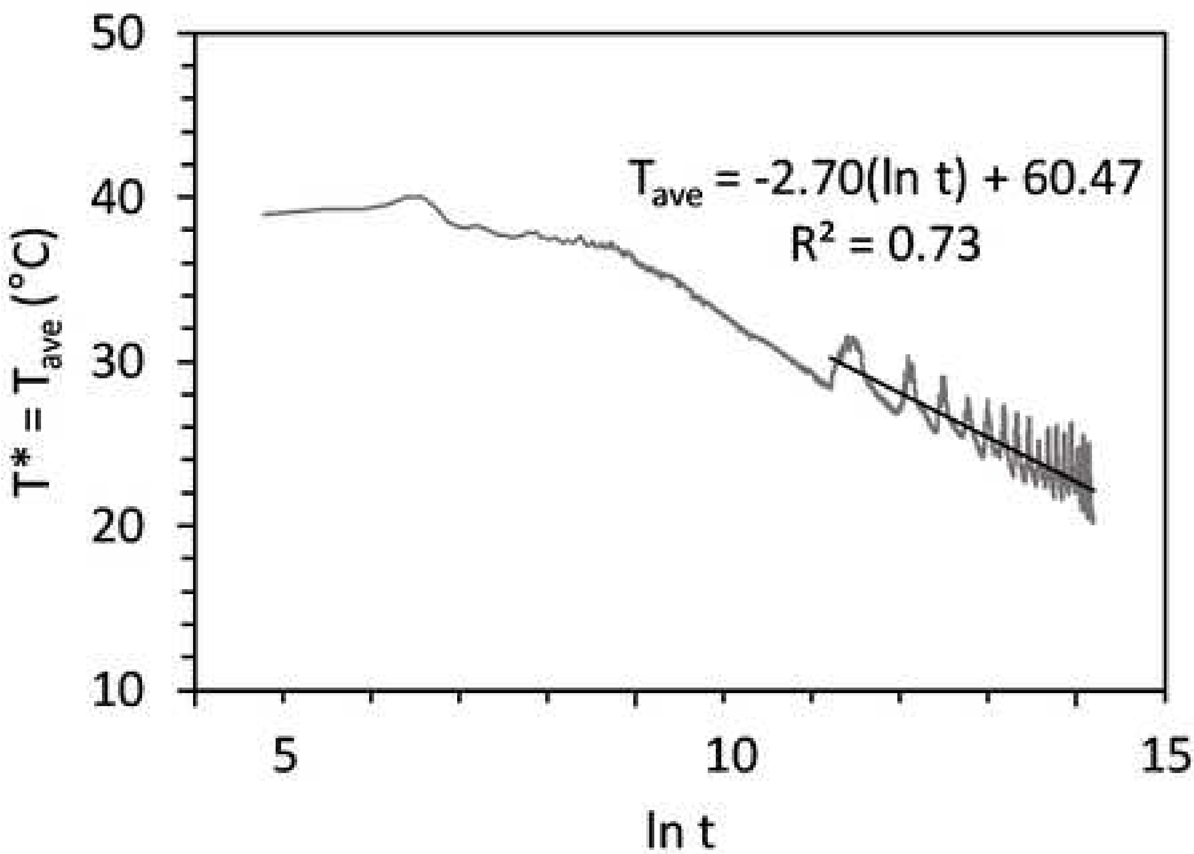

50
40
30
20
10
T* = T_ave (°C)
5
10
15
ln t
T_ave = -2.70(ln t) + 60.47
R² = 0.73

(b)

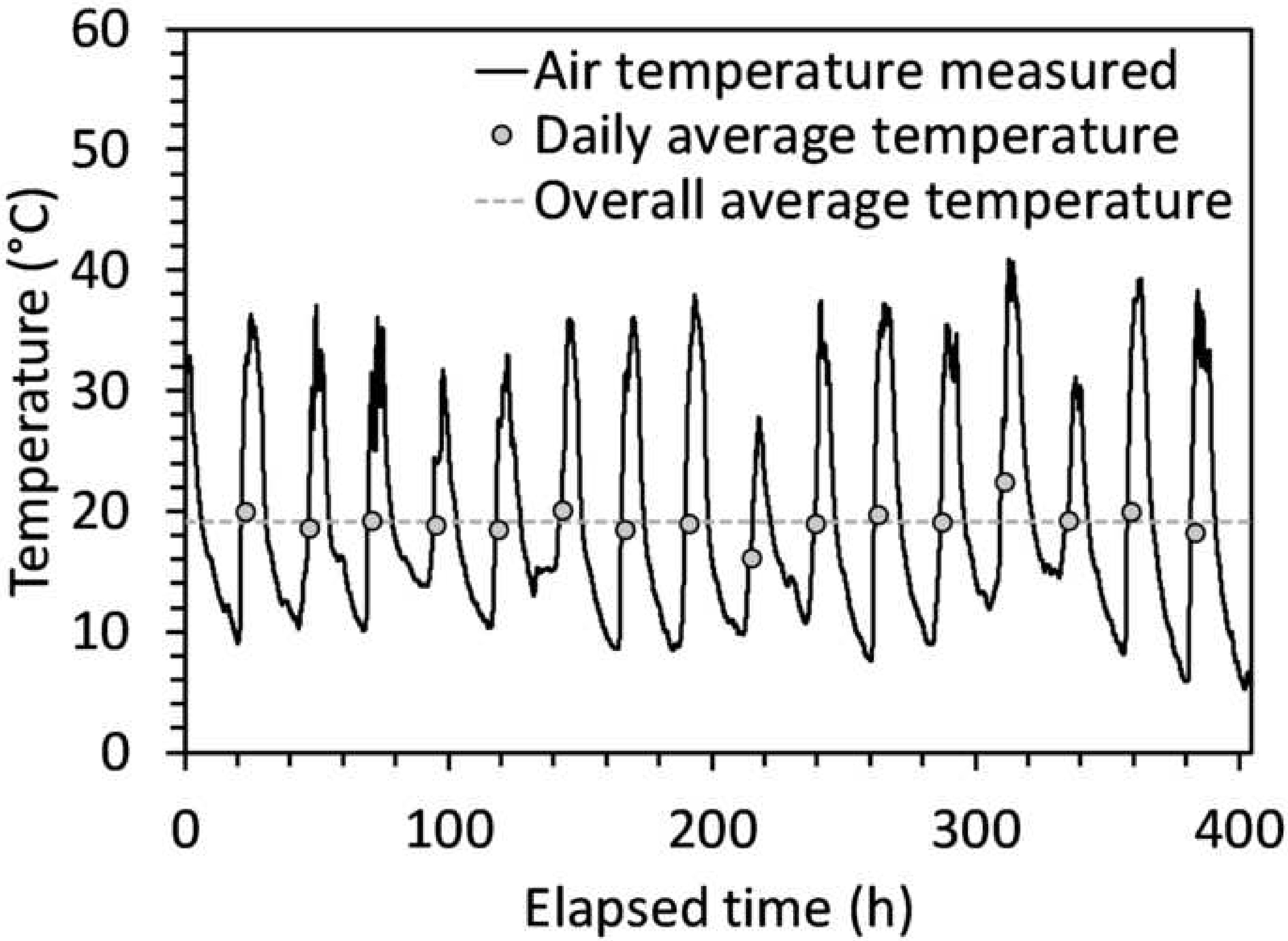
Air temperature measured
Daily average temperature
Overall average temperature
Temperature (°C)
Elapsed time (h)
0
10
20
30
40
50
60
0
100
200
300
400

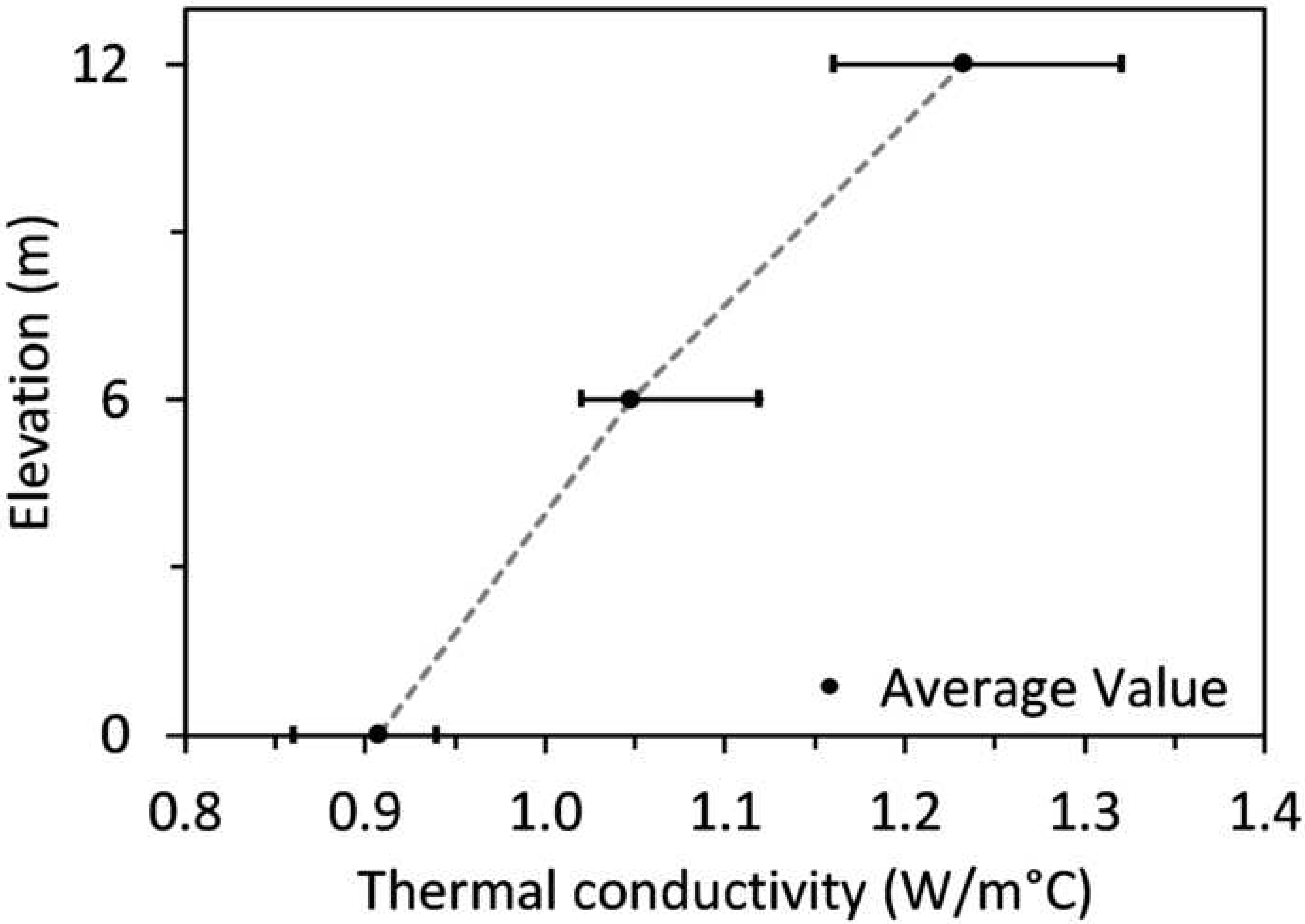
12
6
0
Elevation (m)
0.8
0.9
1.0
1.1
1.2
1.3
1.4
Thermal conductivity (W/m°C)
Average Value